

Article

# Thermoelectric Array Sensors with Selective Combustion Catalysts for Breath Gas Monitoring

Woosuck Shin <sup>1,\*</sup>, Tomoyo Goto <sup>2</sup> , Daisuke Nagai <sup>1</sup>, Toshio Itoh <sup>1</sup>, Akihiro Tsuruta <sup>1</sup>, Takafumi Akamatsu <sup>1</sup> and Kazuo Sato <sup>3</sup>

<sup>1</sup> National Institute of Advanced Industrial Science and Technology (AIST), Shimo-Shidami, Moriyama-ku, Nagoya 463-8560, Japan; d-nagai@aist.go.jp (D.N.); itoh-toshio@aist.go.jp (T.I.); a.tsuruta@aist.go.jp (A.T.); t-akamatsu@aist.go.jp (T.A)

<sup>2</sup> The Institute of Scientific and Industrial Research, Osaka University, Ibaraki 567-0047, Japan; goto@sanken.osaka-u.ac.jp

<sup>3</sup> Department of Mechanical Engineering, Aichi Institute of Technology, Toyota 470-0392, Japan; sato@aitech.ac.jp

\* Correspondence: w.shin@aist.go.jp; Tel.: +81-52-736-7107

Received: 29 March 2018; Accepted: 13 May 2018; Published: 16 May 2018



**Abstract:** Inflammable breath gases such as H<sub>2</sub> and CH<sub>4</sub> are used as bio markers for monitoring the condition of the colon. However, their typical concentrations of below 100 ppm pose sensitivity and selectivity challenges to current gas sensing systems without the use of chromatography. We fabricated a compact, gas-selective thermoelectric array sensor (TAS) that uses micro-machined sensor devices with three different combustion catalysts to detect gases such as H<sub>2</sub>, CO, and CH<sub>4</sub> in breath. Using Pt/Pt-W thin-film micro-heater meanders, Pd/Al<sub>2</sub>O<sub>3</sub>, Pt,Pd,Au/Co<sub>3</sub>O<sub>4</sub>, and Pt/Al<sub>2</sub>O<sub>3</sub> catalysts were heated to 320, 200, and 125 °C, respectively, and the gas sensing performances of the TAS for each gas and for a model breath gas mixture of 100 ppm H<sub>2</sub>, 25 ppm CO, 50 ppm CH<sub>4</sub>, and 199 ppm CO<sub>2</sub> in air were investigated. Owing to its high catalyst temperature, the Pd/Al<sub>2</sub>O<sub>3</sub> catalyst burned all three gases, while the Pt,Pd,Au/Co<sub>3</sub>O<sub>4</sub> burned CO and H<sub>2</sub> and the Pt/Al<sub>2</sub>O<sub>3</sub> burned H<sub>2</sub> selectively. To calibrate the gas concentration of the mixture gas without the use of a gas separation tool, linear discriminant analysis was applied to measure the sensing performance of TAS. To enhance the gas selectivity against H<sub>2</sub>, a double catalyst structure was integrated into the TAS sensor.

**Keywords:** thermoelectric device; array sensor; H<sub>2</sub>; CO; CH<sub>4</sub>; combustion catalyst; micro-electromechanical systems (MEMS)

## 1. Introduction

Human breath is a highly complex mixture of more than 100 types of gases, including NO, CO<sub>2</sub>, CO, NH<sub>4</sub>, CH<sub>4</sub>, H<sub>2</sub>, and various volatile organic components (VOCs), many of which can provide useful information in the monitoring of the human health condition [1]. H<sub>2</sub> and CH<sub>4</sub> are generated in the human body by the fermentative reaction of bacteria, enabling the evaluation of the digestive and absorptive functions in the intestine based on measurements of these gases in exhaled breath [2]. CO is exhaled by smokers and has been reported as a marker gas for various diseases [1,3].

The techniques developed for the detection and measurement of breath gases can be generally categorized into two major groups: (1) conventional analyzers that use gas chromatography (GC) coupled with mass spectroscopy (MS) or flame ionized detection (FID) [4], recently developed ion mobility spectrometry (IMS) [5] and proton-transfer-reaction (PTR) [6] technologies, and rather simple systems comprising GCs coupled to metal oxide (MOX) sensors; and (2) e-Nose systems, which are

commonly constructed as single [7] or array sensors [8]. Although the development of e-Nose systems has been steady over the past few decades, multi-gas sensors for breath gas detection have yet to emerge. Two major stumbling blocks have been the ability to detect specific gases selectively using a single sensing element and the ability to detect gas precisely in humid conditions.

Low-cost devices for breath analysis without the use of gas chromatography require the use of highly selective and sensitive sensors. Previous studies reported the development of various gas sensors, including semiconducting MOX sensor arrays [9] and micro-hotplate-based gas sensor arrays [10,11]. For the specific analysis of CO and CH<sub>4</sub> gas mixtures, a micromachined gas sensor based on a catalytic thick film/SnO<sub>2</sub> thin-film bilayer and a thin-film heater has been developed [12]. Recently, a thermoelectric gas sensor (TGS) based on a synergetic combination of catalytic combustion and thermoelectric conversion has been developed for the detection of H<sub>2</sub> [13]. Using TGS-based techniques, a gas-flow-type prototype for the selective monitoring of H<sub>2</sub> in breath gas has been developed and tested [14] and an integrated multi-TGS sensor comprising three thermoelectric array devices with ceramic catalysts for the combustion of CH<sub>4</sub>, CO, and H<sub>2</sub> has been developed and its performance in detecting these gases at 5000 ppm has been preliminarily tested [15]. Although the detection of the CO and CH<sub>4</sub> ppm levels was not easy in these studies, the authors have subsequently succeeded in measuring both gases down to 1 ppm [16–18]. However, measuring the ppm levels of gas using a single micro-chip-type device remains challenging, with many technical, drift, and process problems remaining, as the extreme fragility of the sensor membranes leads to a low process yield in developing multi-sensor chips with four clean membranes.

In this study, we improved the sensitivity of a thermoelectric array gas sensor (TAS) by applying the working principle of a TGS with different combustion catalysts for the simultaneous detection of CO, H<sub>2</sub>, and CH<sub>4</sub> without gas separation to low-concentration gases at several ppm levels. We investigated the performance of this sensor in an environment of simulated breath gases including water and CO<sub>2</sub>. Our results suggest that the proposed improved TAS is a promising candidate for application as a simple, low-cost breath gas analyzer.

## 2. Experimental

### 2.1. Integration of Catalyst Combustor onto Array Sensor

Figure 1 shows the catalyst deposition process and a photo of the proposed TAS device, which comprises a 6 mm × 6 mm chip containing four thermoelectric device sensors. The sensors are fabricated in a p-type B-doped SiGe pattern and a Pt/Pt-W multilayer micro-heater meander pattern and incorporate combustion catalysts integrated onto a Si<sub>3</sub>N<sub>4</sub>-SiO<sub>2</sub> multilayer membrane on a double-side polished Si substrate. The B-doped SiGe thin film is prepared using a helicon sputtering method (i-sputter, ULVAC, Inc., Kanagawa, Japan). The thin micro-heater meander films are multi-layer sputter depositions of a 10-nm-thick Ta adhesion layer, a 200-nm-thick Pt layer, and a 10-nm-thick Pt-W layer, and are patterned using a lift-off process. The reverse side of the Si substrate is etched out using an aqueous KOH solution to prepare the membrane structure. Details on the processing and patterning of the SiGe thin film were previously reported in [11].

Pt/Al<sub>2</sub>O<sub>3</sub>, Pt,Pd,Au/Co<sub>3</sub>O<sub>4</sub>, and Pd/Al<sub>2</sub>O<sub>3</sub> combustion catalysts with metal contents of 30, 3, and 10 wt %, respectively, are used for the detection of H<sub>2</sub>, CO, and CH<sub>4</sub>, respectively. The Pt/Al<sub>2</sub>O<sub>3</sub> and Pd/Al<sub>2</sub>O<sub>3</sub> catalysts are prepared by mixing an aqueous solution dispersed with a colloid of noble metal particles (Tanaka Kikinzoku Kogyo K.K.; mercaptosuccinic acid, with metal content 4 wt % and average particle diameter 3 nm) and a commercial alumina powder (Taimai Chemicals Co., Ltd., Tokyo, Japan; average particle diameter 100 nm). The Pt,Pd,Au/Co<sub>3</sub>O<sub>4</sub> catalyst is prepared by mixing an aqueous solution dispersed with the above colloid, as well as a colloid of Au metal particles (Tanaka Kikinzoku Kogyo K.K.; mercaptosuccinic acid, Au content 2 wt %, average particle diameter 3 nm) and a commercial cobalt oxide (Co<sub>3</sub>O<sub>4</sub>) powder (Aldrich; average particle diameter 20–30 nm). The mixture solution is stirred at a temperature of 100, 90, and 70 °C, respectively, until the

water evaporates and the solid residue is baked again in air at 300 °C for 2 h to obtain powder catalysts, which are mixed with an organic vehicle (a mixture of terpineol and ethyl cellulose) to form ceramic pastes. The pastes are integrated onto the thin membrane of the TAS using an air dispenser (Musashi Engineering Inc., Tokyo, Japan), and the TAS is then baked in air at 300 °C for 2 h. The size of the catalyst is constrained to a diameter of 0.4 mm, or about 61% of the diameter of a single sensor [13]. After package dicing, the catalysts are deposited onto the TAS device and wire-bonded onto a ceramic package comprising 28 electrode pads (Kyocera Co., Kyoto, Japan, Ceramic Packages for MEMS Sensors).

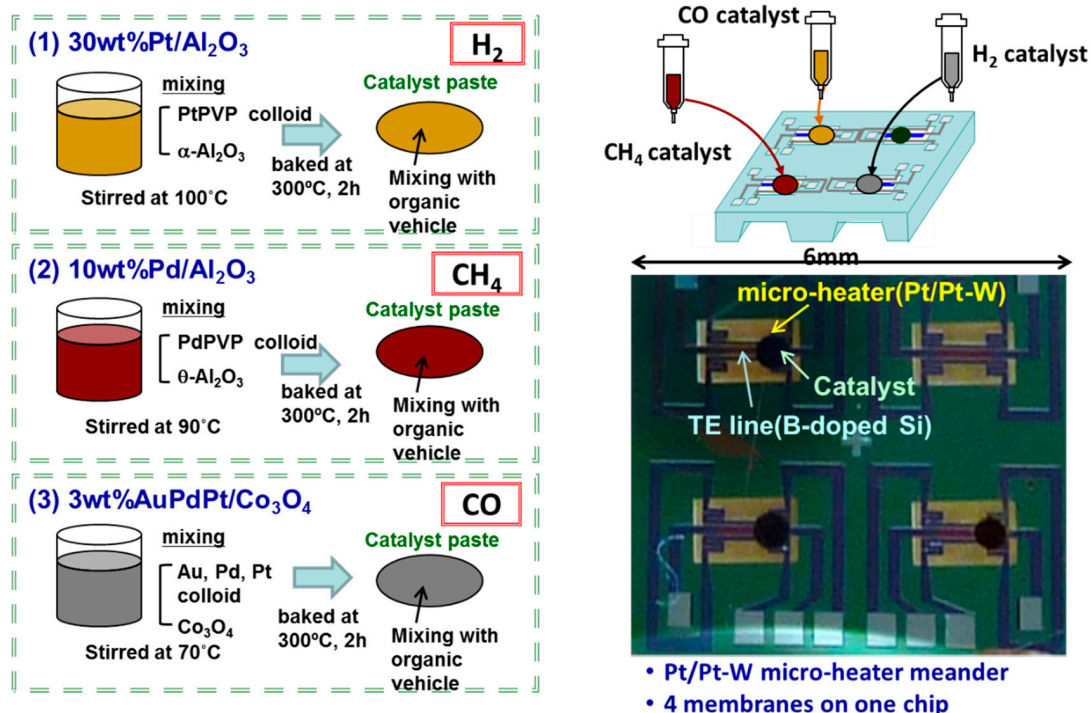


**Figure 1.** Catalyst combustors deposited onto Pt/Al<sub>2</sub>O<sub>3</sub>, Pd/Al<sub>2</sub>O<sub>3</sub>, and Au/Co<sub>3</sub>O<sub>4</sub> array sensor devices for the gas detection of H<sub>2</sub>, CH<sub>4</sub>, and CO, respectively.

## 2.2. Sensor Response Test

The gas response performance of the device was investigated using a gas-flow-type test chamber. The voltage signal from the TAS was recorded by alternately flowing a dry target gas mixture and dry air into the test chamber at a flow rate of 200 mL/min. Performance testing of the TAS was carried out using two types of gas mixture: (1) single gas mixtures of H<sub>2</sub>, CO, or CH<sub>4</sub> in air; and (2) multiple gas mixtures of H<sub>2</sub> + CO + CH<sub>4</sub> in air. The single gases were mixed at 0–100 ppm, while the multiple gases were mixed in the ratio H<sub>2</sub>:100/CO:25/CH<sub>4</sub>:50/CO<sub>2</sub>:199 (ppm). The composition ratio of the test gas is determined to simulate the maximum concentration of three inflammable gases in breath, and the reference gas of the CO<sub>2</sub> level is fitted to the H<sub>2</sub> concentration. Details on the gas concentrations in breath has been reported previously [2], which is one hundred times lower than the concentration found in the human colon [19].

To measure the gas combustion-induced catalyst temperature change, the surface temperature of the catalyst was monitored using an IR camera that had previously been calibrated using thermocouples. In contrast to our previous experiments, it was difficult to read temperature change using the IR camera, which reflected the differences in concentrations: in the previous experiments, concentrations of hydrogen gas in air as high as 1.0% were measured, leading to catalyst temperature increases of 40 °C; by contrast, the current experiments involved temperature changes as low as 0.005 °C for hydrogen concentrations of 1 ppm.

### 3. Results and Discussion

#### 3.1. Combustion Performance of Pt/Al<sub>2</sub>O<sub>3</sub>, Pt,Pd,Au/Co<sub>3</sub>O<sub>4</sub>, and Pd/Al<sub>2</sub>O<sub>3</sub> Catalysts

The combustion performance of the Pt/Al<sub>2</sub>O<sub>3</sub>, Pt,Pd,Au/Co<sub>3</sub>O<sub>4</sub>, and Pd/Al<sub>2</sub>O<sub>3</sub> catalysts can be estimated based on the voltage signal of the TAS ( $\Delta V$ ), which is linearly proportional to the increase in the temperature ( $\Delta T$ ) as a result of the gas combustion on the catalyst:

$$\Delta V = \alpha \Delta T$$

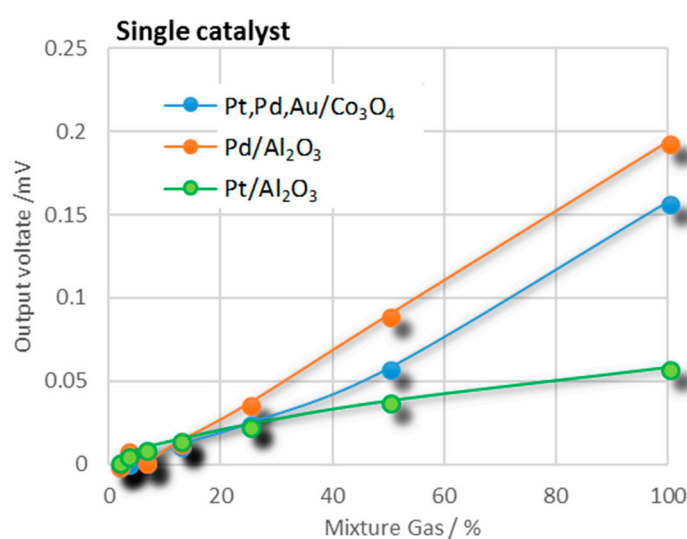
where  $\alpha$  is the Seebeck coefficient of a thermoelectric film of boron-doped Si<sub>0.8</sub>Ge<sub>0.2</sub>.

Table 1 lists the voltage signals,  $\Delta V$ , produced by the respective TAS catalysts for three inflammable single gases at concentrations of 100 ppm. The sensor operational temperatures—that is, the catalyst temperatures at which the best performances were produced in our previous study [16]—are increased to 150 °C for H<sub>2</sub> and decreased to 200 and 320 °C, respectively, for CO and CH<sub>4</sub>. Figure S1 in the Supplementary Material shows the typical response curves (in terms of  $\Delta V$  with respect to time) of the Pd/Al<sub>2</sub>O<sub>3</sub>-catalyst TAS at various gas concentrations of CH<sub>4</sub> in air with the air flow switched to the gas mixture flow at an elapsed time of 100 s and then switched back to air at 200 s.

**Table 1.** Combustion performance of sensors with different catalyst materials separately exposed to single inflammable gases H<sub>2</sub>, CH<sub>4</sub>, and CO at air concentrations of 100 ppm. The sensors were heated separately to avoid interference.

Catalyst Material	Catalyst	$\Delta V$ for Single Gas at 100 ppm (mV)		
	Temp. (°C)	H <sub>2</sub>	CH <sub>4</sub>	CO
Pt/Al <sub>2</sub> O <sub>3</sub>	125	0.036	0.001	0.016
Pt,Pd,Au/Co <sub>3</sub> O <sub>4</sub>	200	0.056	0.001	0.053
Pd/Al <sub>2</sub> O <sub>3</sub>	320	0.085	0.146	0.088

Figure 2 shows the detection performances of the Pt/Al<sub>2</sub>O<sub>3</sub>, Pt,Pd,Au/Co<sub>3</sub>O<sub>4</sub>, and Pd/Al<sub>2</sub>O<sub>3</sub>-catalyst TASs for a H<sub>2</sub>:100 ppm/CO:25 ppm/CH<sub>4</sub>:50 ppm/CO<sub>2</sub>:199 ppm gas mixture at various concentrations in air.



**Figure 2.** Gas responses or calibration curves of three TAS catalyst sensors for mixture gas with relative component concentrations of H<sub>2</sub> 100 ppm, CO 25 ppm, CH<sub>4</sub> 50 ppm, and CO<sub>2</sub> 199 ppm in air. The x-axis represents the concentration of the mixture gas diluted by air.

From Table 1, the Pt/Al<sub>2</sub>O<sub>3</sub> catalyst TAS had a combustion performance of  $\Delta V = 0.036$  mV for 100 ppm H<sub>2</sub> at a catalyst temperature of 125 °C. At this temperature, CO was also burned by this catalyst with a  $\Delta V$  of 0.016 mV for 100 ppm CO. However, the catalyst did not burn CH<sub>4</sub>. From Figure 2, it is seen that the Pt/Al<sub>2</sub>O<sub>3</sub> catalyst burned the CO + H<sub>2</sub> + CH<sub>4</sub> gas mixture more effectively than it burned any of the gases separately. At concentrations above approximately 50%, the gas mixture  $\Delta V$  exceeded the sum of the values (0.05 mV) of the individual gases at 125 °C, with the  $\Delta V$  value for the 25 ppm CO in the gas mixture approximately corresponding to that achieved by the 100 ppm CO single gas.

In our previous studies of Pt/Al<sub>2</sub>O<sub>3</sub> catalysts on micro devices, we found that CO adsorption on the catalyst surface prohibited the combustion of H<sub>2</sub> at lower temperatures [18], making it necessary to increase the catalyst temperature to burn out the adsorbed CO to activate the catalyst surface. This enhanced combustion of CO could be explained in terms of activation with coexisting H<sub>2</sub>, and these results were used to obtain operating temperatures of 320, 200, and 125 °C, respectively, for Pd/Al<sub>2</sub>O<sub>3</sub>, Pt,Pd,Au/Co<sub>3</sub>O<sub>4</sub>, and Pt/Al<sub>2</sub>O<sub>3</sub>-catalyst TAS devices. The Pt,Pd,Au/Co<sub>3</sub>O<sub>4</sub>-catalyst TAS produced a  $\Delta V$  of 0.53 mV in burning 100 ppm CO at a catalyst temperature of 200 °C and 0.56 mV in burning 100 ppm H<sub>2</sub>, but could not burn CH<sub>4</sub>. The  $\Delta V = 0.158$  mV obtained by burning the H<sub>2</sub> + CO + CH<sub>4</sub> gas mixture in air at 200 °C was greater than the sum of the  $\Delta V$  values (0.0825 mV) obtained by burning the single gases separately at the same temperature.

The Pd/Al<sub>2</sub>O<sub>3</sub> catalyst burned all three gases at a catalyst temperature of 320 °C, producing nearly identical values of  $\Delta V$  for H<sub>2</sub> and CO, but a value approximately twice that for CH<sub>4</sub>. At catalyst temperatures above 350 °C, the combustion of CH<sub>4</sub> by the catalyst increased to even higher values relative to that with CO. The CH<sub>4</sub> selectivity,  $S_{CO/CH_4} = \Delta V_{CO} / \Delta V_{CH_4}$ , at a catalyst temperature of 360 °C, was 0.5. At a catalyst temperature of 320 °C, the TAS sensor was able to detect CO and CH<sub>4</sub> down to a 1-ppm concentration level. However, several technical problems were encountered: the base line of the sensor voltage signal was unstable and drifted, and the linearity of  $V$  with respect to gas concentration became worse.

### 3.2. Double Catalyst to Enhance TAS Gas Selectivity

As demonstrated in Table 1 and Figure 2, linear discriminant analysis (LDA) could be applied in assessing combustion performance. However, the gas selectivity of TAS is low, particularly for CO and CH<sub>4</sub>, and we therefore attempted to control the selectivity of these gases using a “double catalyst structure” [8,19] to adjust the balance of the combustion heats of the catalysts deposited onto the thermoelectric film in the micro-TGS devices to obtain further improvements in TAS selectivity.

As shown in Figure 3, single and double 30 wt % Pt/ $\alpha$ -Al<sub>2</sub>O<sub>3</sub> catalysts were deposited onto the cold ends of separate thermoelectric patterns to produce two new TAS types (B and C, respectively, with type-A indicating the original TAS configuration). Here, the hot side indicates the location of the combustion catalyst, while the counter or cold side refers to the position of the additional catalyst on the membrane.

As an example of the effects of the double catalyst process, the deposition of the Pt,Pd,Au/Co<sub>3</sub>O<sub>4</sub> catalyst (at point A) should allow for the oxidization of both H<sub>2</sub> and CO. Depositing Pt/ $\alpha$ -Al<sub>2</sub>O<sub>3</sub>, which is a combustion catalyst for H<sub>2</sub> [13], onto the other side of membrane (point B) should reduce the temperature difference between points A and B owing to the combustion heat of the Pt/ $\alpha$ -Al<sub>2</sub>O<sub>3</sub>. As a result, introducing a mixture of H<sub>2</sub> and CO into this calorimetric-TGS device will inhibit the sensor response of the Pt,Pd,Au/Co<sub>3</sub>O<sub>4</sub> catalyst to H<sub>2</sub>.

The response  $\Delta V$  values of A-, B-, and C-type TASs were measured for single and mixture gases. Because of the CO absorption on the Pt/Al<sub>2</sub>O<sub>3</sub> catalyst, the driving temperature of the Pt/Al<sub>2</sub>O<sub>3</sub> catalyst was increased to 150 °C to enable burning the CO. Figure 4 shows the responses of the three TAS types for a H<sub>2</sub> 100 ppm, CO 25 ppm, CH<sub>4</sub> 50 ppm, and CO<sub>2</sub> 199 ppm gas mixture in air, which can be used for calibration curves. The responses for single and mixture gases are listed in Table 2.

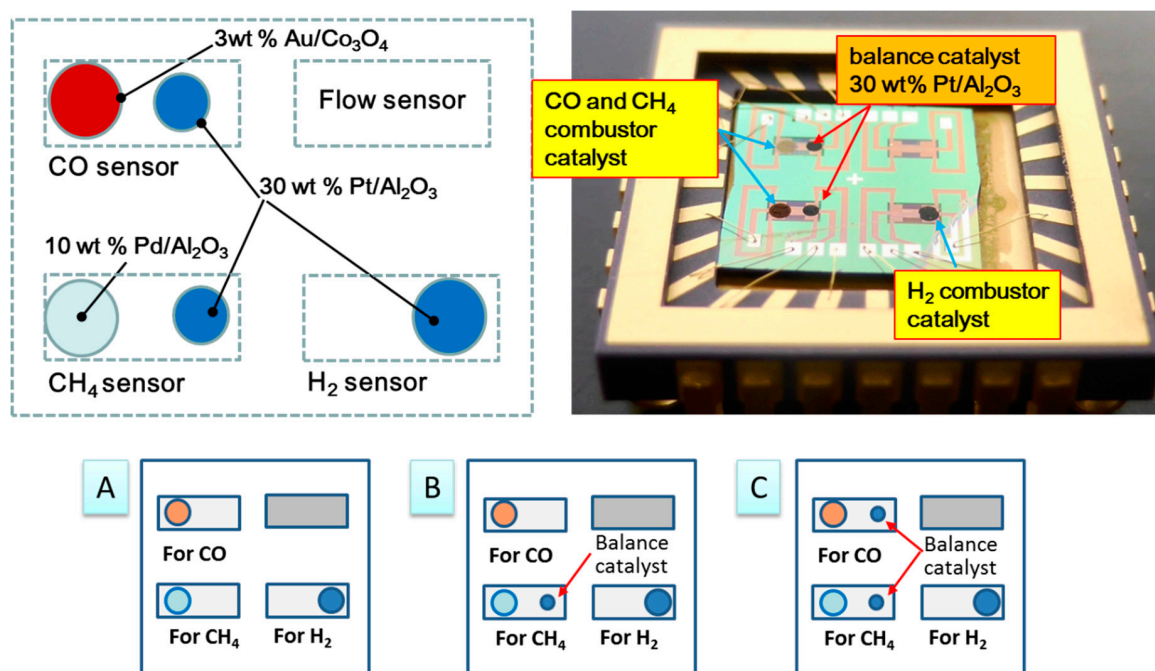


**Figure 3.** Additive deposition of 30 wt % Pt/ $\alpha$ -Al<sub>2</sub>O<sub>3</sub> catalyst, which combusts H<sub>2</sub> gas to enhance gas selectivity. (A) Schematic of C-type TAS; (B) Following package dicing, catalysts are deposited onto the TAS device and wire-bonded onto a ceramic package; (C) Positioning of additive 30 wt % Pt/ $\alpha$ -Al<sub>2</sub>O<sub>3</sub> catalyst for type-B and -C TASs.

**Table 2.** Combustion performance of TASs without/with double catalyst structure (A/B and C, respectively) and different catalyst materials for single inflammable gases H<sub>2</sub>, CH<sub>4</sub>, and CO at 200 ppm/air and for gas mixtures.

Single Catalyst Type A						
Catalyst	Single Gas 100 ppm			Mix Gas (%)		
	H <sub>2</sub>	CH <sub>4</sub>	CO	25	50	100
Pt/Al <sub>2</sub> O <sub>3</sub>	0.0386	0.0034	0.0256	0.016	0.036	0.055
Pd/Al <sub>2</sub> O <sub>3</sub>	0.142	0.164	0.082	0.18	0.229	0.33
Pt,Pd,Au/Co <sub>3</sub> O <sub>4</sub>	0.0307	0.12	0.083	0.025	0.078	0.158
One Double Catalyst Type B						
Catalyst	Single Gas 100 ppm			Mix Gas (%)		
	H <sub>2</sub>	CH <sub>4</sub>	CO	25	50	100
Pt/Al <sub>2</sub> O <sub>3</sub>	0.230	0.000	0.033	0.025	0.078	0.158
Double	0.125	0.176	0.027	0.086	0.136	0.226
Pt,Pd,Au/Co <sub>3</sub> O <sub>4</sub>	0.045	0.003	0.055	0.016	0.036	0.055
Two Double Catalyst Type C						
Catalyst	Single Gas 100 ppm			Mix Gas (%)		
	H <sub>2</sub>	CH <sub>4</sub>	CO	25	50	100
Pt/Al <sub>2</sub> O <sub>3</sub>	0.150	−0.030	−0.030	0.023	0.0668	0.134
Double	0.092	0.146	−0.003	0.108	0.149	0.229
Double	0.110	0.120	0.260	0.0232	0.0485	0.152

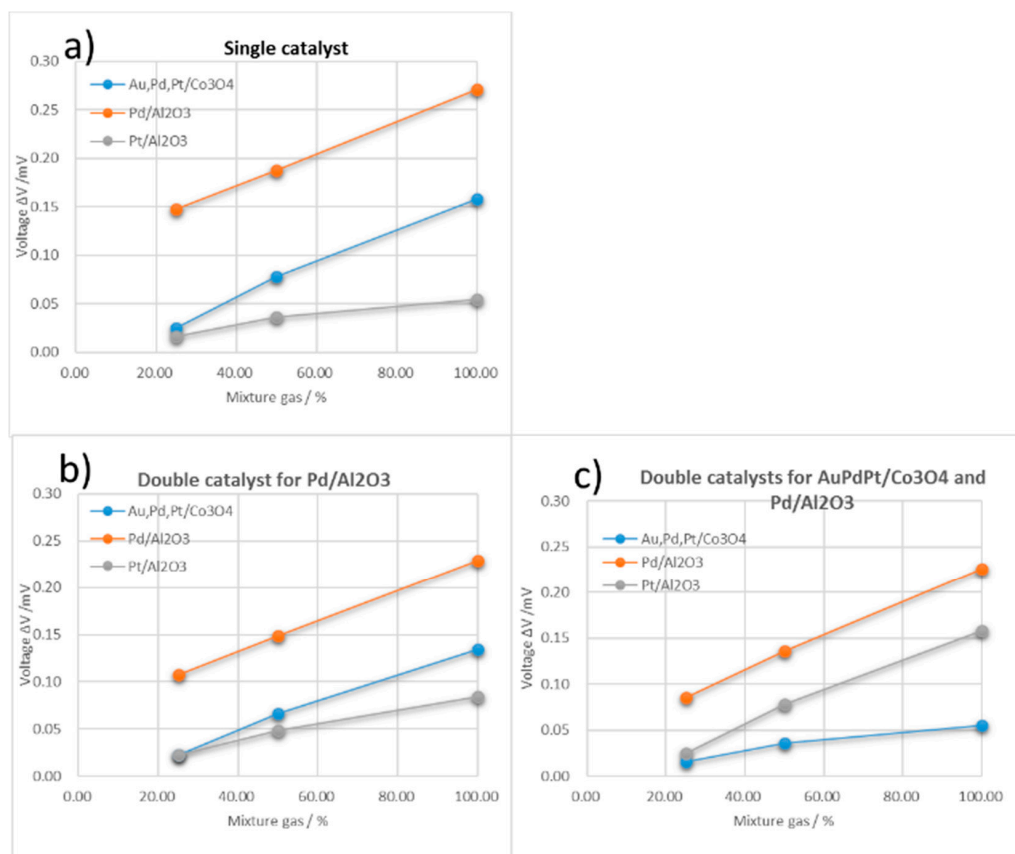


**Figure 4.** Gas responses or calibration curves of TASs of types (a–c) for a mixture gas with relative component concentrations of H<sub>2</sub> 100 ppm, CO 25 ppm, CH<sub>4</sub> 50 ppm, and CO<sub>2</sub> 199 ppm in air. The x-axis represents the concentration of the air-diluted mixture gas.

Figure 4a shows the mixture-gas response for the type-A TAS, which as noted above, has the same structure as the TAS discussed in the preceding sections. Unsurprisingly, the reaction is very similar to that shown in Figure 2, although the  $\Delta V$  values produced by the methane and CO sensors are higher; this difference can be attributed to the catalyst size difference between the respective devices, with the larger  $\Delta V$  representing a response to a larger signal.

Figure 4b shows the response of the type-B TAS, which has a double catalyst in its CH<sub>4</sub> sensor, to the gas mixture. Although the response is essentially the same as that of the type-A TAS, the methane sensor in the former has a lower  $\Delta V$  than the sensor in the former. This reduced  $\Delta V$  can be attributed to the combustion of H<sub>2</sub> and CO gas on the Pt/Al<sub>2</sub>O<sub>3</sub> catalyst on the type-B methane catalyst. As seen in Figure 4c, this double catalyst effect becomes more prominent in the CO sensor of the type-C TAS with double catalysts of Pt,Pd,Au/Co<sub>3</sub>O<sub>4</sub> and Pt/Al<sub>2</sub>O<sub>3</sub>. While the  $\Delta V$  for the mixture gas of the CO catalyst of the type-A TAS is equal to the sum of the  $\Delta V$  values of each single gas, the mixture gas response of the type-C catalyst is close to that for 25 ppm CO in air, i.e., the catalyst is CO selective. The CH<sub>4</sub> sensor of the type-C TAS produces similar response levels, demonstrating the effect of the double catalyst.

While all of the methane sensor responses increase linearly with gas concentration ( $R^2 > 0.998$ ), the linearities of the CO ( $R^2 > 0.995$ ) and H<sub>2</sub> sensors ( $R^2 > 0.956$ ) are lower and the increases in their  $\Delta V$  values decline in the lower ppm ranges. Based on this linear performance of the sensors, LDA analysis was applied to the sensing performance factors shown in Table 2 and Figure 4 to evaluate and distinguish the composition of the mixture gas.

The method for using multivariate analysis and calibration models built individually for each type of sensor based on the previously identified single-gas responses is illustrated in Figure 5, where Sn

represents the parameters extracted from the response signals of the respective sensors ( $n = 1, 2, 3$ ) and  $a, b, c$  are coefficients indicating the respective gas components. The sensor responses are normalized to that for a 100-ppm single gas in air—for example,  $S_1 = a_1x + b_1y + c_1z$ . The coefficients of the gas composition equation can then be calculated under a simple assumption that the mixed gas  $\Delta V$  is the sum of the single gas response signals. As the immunity of TGS to water vapor has been validated many times [13,14] and demonstrated in the hospital [20], the effect of water vapor can be ignored. The results for the three TAS types for different mixture gas compositions are listed in Table 3. The validity of the proposed method is validated by the closeness of these coefficients to the original mixture gas compositions.

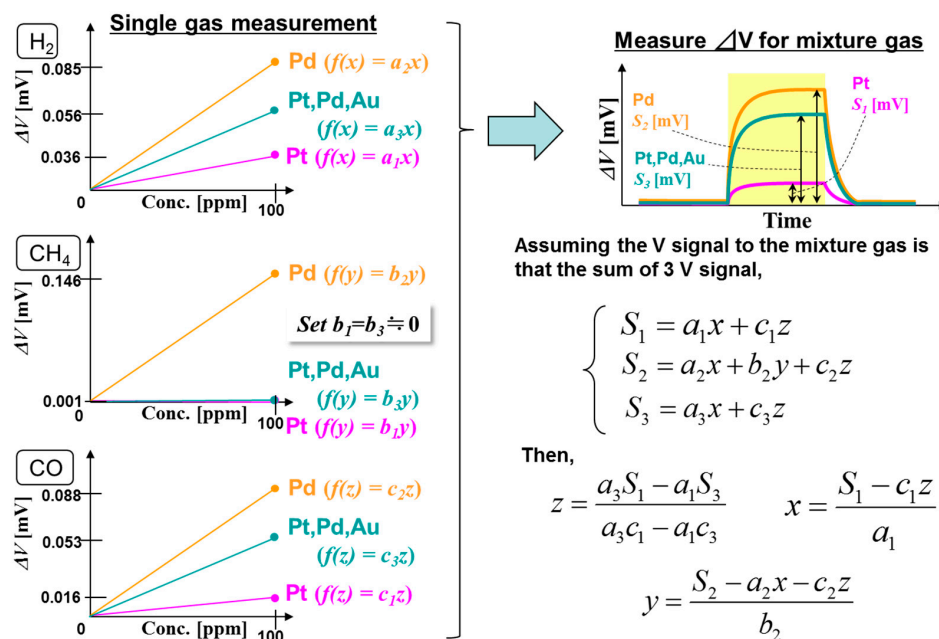


Figure 5. Schematic of the linear analysis method used in this work.

Table 3. Gas concentration for three TAS types by mixture gas composition.

	Type A	Type B	Type C	Mixture Gas Composition
H <sub>2</sub> conc. (x)	121	62	108	100 ppm
CH <sub>4</sub> conc. (y)	86	77	89	50 ppm
CO <sub>2</sub> conc. (z)	21	46	−4	25 ppm

Using data on the linear relation of  $V$  to gas concentration, calibration can be applied to adjust the gas concentration, for example, from 86 to 50 ppm CH<sub>4</sub> for the type-A TAS. This can provide simple gas composition estimates if the sensor response is stable throughout the calibration process and in actual use. The effect of H<sub>2</sub> combustion as a result of the double catalyst effect can be further used to modify the responses of the types-B and -C TASs, as shown in Figure 5. However, the linear equation analysis returns a negative CO gas composition for the type-C TAS, making it difficult to adjust the gas composition in this case, and reflecting the need of further modification and improvement of the double catalyst method for the Pt,Pd,Au/Co<sub>3</sub>O<sub>4</sub> and Pt/ $\alpha$ -Al<sub>2</sub>O<sub>3</sub> CO sensor. The type-B TAS estimates relatively low H<sub>2</sub> concentrations, which results in relatively high CH<sub>4</sub> and CO responses. These results suggest that the type-A TAS is most suitable for discriminating separate gas compositions using linear analysis, while the double catalyst types-B and -C TASs require further modification in terms of, for example, catalyst size or temperature, even though both sensors have enhanced selectivity against H<sub>2</sub>.

We are currently developing a breath detection system based on the use of a TAS structure for which the linear modeling results of this study will be potentially useful in calibrating the sensors in operating mode. As the sensor response changes as a result of altered installation packages or gas flow, the linear calibration method demonstrated in this study can be used to explore, test, and calibrate the performance of new array sensor packages with respect to specific operating modes. However, such calibration challenges can also be overcome by combining sensors into an array (e.g., E-nose) in which differences in selectivity are exploited through statistical analysis. Further work needs to be carried out, the calibration for the accuracy of the gas concentration with the estimation error analysis is necessary, and the cross-validation with human breath, including the interference of gas mixtures of very low concentration analytes, should be tested carefully, for instance, acetone, which is of several ppm in breath gas of diabetes.

#### 4. Conclusions

TASs based on Pd/Al<sub>2</sub>O<sub>3</sub>, Pt,Pd,Au/Co<sub>3</sub>O<sub>4</sub>, and Pt/Al<sub>2</sub>O<sub>3</sub> combustion catalysts were developed and assessed in terms of selective breath gas detection performance for the inflammable gases H<sub>2</sub>, CO, and CH<sub>4</sub> at a variety of concentrations. Sensors of each catalyst type were fabricated as micro-machined membranes and heated using Pt/Pt-W thin film heaters to 320 °C (Pd/Al<sub>2</sub>O<sub>3</sub>), 200 °C (Pt,Pd,Au/Co<sub>3</sub>O<sub>4</sub>), and 125 °C (Pt/Al<sub>2</sub>O<sub>3</sub>), with the gas concentrations detected via the thermoelectric conversion of combustion heat to a Seebeck voltage in linear proportion to the gas concentration.

The TAS responses for the single composition gases were evaluated separately and the responses for mixture gases were tested to confirm that the sensors could detect the concentrations of the three gases selectively and linearly. To enhance the limited gas selectivity against H<sub>2</sub>, a double catalyst structure was integrated into the sensor membrane, which was shown to be effective in enhancing the sensor performance and enabling a more favorable sensor design.

Based on this linearization of combined measurement results, it is possible to estimate the concentrations of individual gases using a TAS, which could facilitate the simpler screening of lung cancer patients and monitoring of breath gas concentrations. In future research, we will seek to improve the sensitivity of the proposed thermoelectric multi gas sensor to gases at concentrations at the several ppm level and to investigate the performance of this enhanced sensor in measuring simulated real-environment gases such as water and CO<sub>2</sub>. We believe that the sensor developed in this study represents a promising candidate for use in a simple, low-cost breath gas analyzer.

**Supplementary Materials:** The following are available online at <http://www.mdpi.com/1424-8220/18/5/1579/s1>, Figure S1: Gas response curves of the TAS with Pd/Al<sub>2</sub>O<sub>3</sub> catalysts for the various concentration of CH<sub>4</sub> in air.

**Author Contributions:** W.S. designed the device and fabrication process, and wrote the paper; T.G., D.N., A.T., and T.A. processed the catalyst, thermoelectric device, and sensor devices, and performed the gas response experiments; T.I. conceived of and designed the data analysis; performed the gas response experiments; K.S. designed the device operating condition; All authors discussed the results and the implications of this manuscript.

**Acknowledgments:** We are grateful to AIST Laboratory members, Michi Yamaguchi, Atsuko Hotta, and Takaomi Nakashima for their technical support in the preparation of the devices and sensor tests used in this study, and Maiko Nishibori of Kyushu University Japan for her comments on this study. This work has been supported in part by the “Development Project for Extremely-Early Diagnostics Technologies for Human Diseases” of Aichi Prefecture, Japan.

**Conflicts of Interest:** The authors declare no conflict of interest.

#### References

1. Philips, M.; Herrera, J.; Krishnan, S.; Zain, M.; Greenberg, J.; Cataneo, R.N. Variation in volatile organic compounds in the breath of normal humans. *J. Chromatogr.* **1999**, *729*, 75–88. [[CrossRef](#)]
2. Shin, W. Medical applications of breath hydrogen measurements. *Anal. Bioanal. Chem.* **2014**, *406*, 3931–3939. [[CrossRef](#)] [[PubMed](#)]

3. Ohira, S.; Toda, K. Micro gas analyzers for environmental and medical applications. *Anal. Chim. Acta* **2008**, *619*, 143–156. [[CrossRef](#)] [[PubMed](#)]
4. Cao, W.; Duan, Y. Current status of methods and techniques for breath analysis. *Crit. Rev. Anal. Chem.* **2007**, *37*, 3–13. [[CrossRef](#)]
5. Baumbach, J.I.; Eiceman, G.A. Ion Mobility Spectrometry: Arriving On Site and Moving Beyond a Low Profile. *Appl. Spectrosc.* **1999**, *53*, 338A–355A. [[CrossRef](#)] [[PubMed](#)]
6. Herbig, J.; Amann, A. Proton Transfer Reaction-Mass Spectrometry Applications in Medical Research. *J. Breath Res.* **2009**, *3*, 020201–020202. [[CrossRef](#)] [[PubMed](#)]
7. Fleischer, M.; Simon, E.; Rumpel, E.; Ulmer, H.; Harbeck, M.; Wandel, M.; Fietzek, C.; Weimar, U.; Meixner, H. Detection of volatile compounds correlated to human diseases through breath analysis with chemical sensors. *Sens. Actuators B Chem.* **2002**, *83*, 245–249. [[CrossRef](#)]
8. Peng, G.; Tisch, U.; Adams, O.; Hakim, M.; Shehada, N.; Broza, Y.Y.; Billan, S.; Abdah-Bortnyak, R.; Kuten, A.; Haick, H. Diagnosing lung cancer in exhaled breath using gold nanoparticles. *Nat. Nanotechnol.* **2009**, *4*, 669–673. [[CrossRef](#)] [[PubMed](#)]
9. Tomchenko, A.A.; Harmer, G.P.; Marquis, B.T.; Allen, J.W. Semiconducting metal oxide sensor array for the selective detection of combustion gases. *Sens. Actuators B Chem.* **2003**, *93*, 126–134. [[CrossRef](#)]
10. Hong, H.-K.; Shin, H.W.; Park, H.S.; Yun, D.H.; Kwon, C.H.; Lee, K.; Kim, S.-T.; Moriizumi, T. Gas identification using micro gas sensor array and neural-network pattern recognition. *Sens. Actuators B Chem.* **1996**, *33*, 68–71. [[CrossRef](#)]
11. Mitzner, K.D.; Sternhagen, J.; Galipeau, D.W. Development of a micromachined hazardous gas sensor array. *Sens. Actuators B Chem.* **2003**, *93*, 92–99. [[CrossRef](#)]
12. Yaowu, M.; Okawa, Y.; Tajima, M.; Nakai, T.; Yoshitake, N.; Natsukawa, K. Micro-machined gas sensor array based on metal film micro-heater. *Sens. Actuators B Chem.* **2001**, *79*, 175–181.
13. Nishibori, M.; Shin, W.; Houlet, L.F.; Tajima, K.; Izu, N.; Itoh, T.; Murayama, N.; Matsubara, I. New structural design of micro-thermoelectric sensor for wide range hydrogen detection. *J. Ceram. Soc. Jpn.* **2006**, *114*, 853–856. [[CrossRef](#)]
14. Shin, W.; Nishibori, M.; Izu, N.; Itoh, T.; Matsubara, I.; Nose, K.; Shimouchi, A. Monitoring Breath Hydrogen using Thermoelectric Sensor. *Sens. Lett.* **2011**, *9*, 684–687. [[CrossRef](#)]
15. Nishibori, M.; Shin, W.; Izu, N.; Itoh, T.; Matsubara, I. Fabrication of micro-multi-gas sensor for the detection of hydrogen, carbon monoxide and methane in breath. *Sens. Lett.* **2011**, *9*, 773–777. [[CrossRef](#)]
16. Nagai, D.; Nakashima, T.; Nishibori, M.; Itoh, T.; Izu, N.; Shin, W. Thermoelectric gas sensor with CO combustion catalyst for ppm level carbon monoxide Detection. *Sens. Actuators B Chem.* **2013**, *182*, 789–794. [[CrossRef](#)]
17. Nagai, D.; Nishibori, M.; Itoh, T.; Kawabe, T.; Sato, K.; Shin, W. Ppm level methane detection using micro-thermoelectric gas sensors with Pd/Al<sub>2</sub>O<sub>3</sub> combustion catalyst films. *Sens. Actuators B Chem.* **2015**, *206*, 488–494. [[CrossRef](#)]
18. Goto, T.; Itoh, T.; Akamatsu, T.; Sekino, T.; Shin, W. Relationship between the CO sensing performance of micro-thermoelectric gas sensors and characteristics of PtPd/Co<sub>3</sub>O<sub>4</sub> and PtPd/SnO<sub>2</sub> catalysts. *Sens. Actuators B Chem.* **2017**, *243*, 847–955. [[CrossRef](#)]
19. Campbell, J.L.; Brkljača, R.; Taylor, K.M.; Burgell, R.E.; Yao, C.K.; Ward, S.A.; McSweeney, C.S.; Muir, J.G.; Gibson, P.R. A human pilot trial of ingestible electronic capsules capable of sensing different gases in the gut. *Nat. Electron.* **2018**, *1*, 79–87.
20. Sakai, D.; Hirooka, Y.; Kawashima, H.; Ohno, E.; Ishikawa, T.; Suhara, H.; Takeyama, T.; Koya, T.; Tanaka, H.; Iida, T.; et al. Increase in breath hydrogen concentration was correlated with the main pancreatic duct stenosis. *J. Breath Res.* **2018**, *12*, 36004. [[CrossRef](#)] [[PubMed](#)]

